

Inhibition of Tat-mediated Transactivation and HIV-1 Replication by Human Anti-hCyclinT1 Intrabodies*

Received for publication, August 13, 2002, and in revised form, October 24, 2002
Published, JBC Papers in Press, October 24, 2002, DOI 10.1074/jbc.M208297200

Jirong Bai‡, Jianhua Sui‡§, Rui Ying Zhu‡, Aimée St. Clair Tallarico‡, Francesca Gennari‡§, Dongsheng Zhang‡§, and Wayne A. Marasco‡§¶

From the ‡Department of Cancer Immunology & AIDS, Dana-Farber Cancer Institute and §Department of Medicine, Harvard Medical School, Boston, Massachusetts 02115

Human immunodeficiency virus, type 1 (HIV-1) replication requires the interaction of Tat protein with the human cyclinT1 (hCyclinT1) subunit of the positive transcription elongation factor (P-TEFb) complex, which then cooperatively binds to transactivation response element (TAR) RNA to transactivate HIV transcription. In this report, a non-immune human single-chain antibody (sFv) phage display library was used to isolate anti-hCyclinT1 sFvs that could disrupt hCyclinT1-Tat interactions. The N-terminal 272 residues of hCyclinT1, including the entire cyclin domains and the Tat-TAR recognition motif (TRM), that fully support Tat transactivation was used for panning, and of the five unique anti-hCyclinT1 sFvs that were obtained, three bound to the cyclin box domains and two bound to TRM. All sFvs could be expressed as intrabodies at high levels in transiently transfected 293T and in stable Jurkat and SupT1 transfectants and could specifically co-immunoprecipitate co-expressed hCyclinT1 in 293T cells with varying efficacy without disrupting hCyclinT1-Cdk9 interactions. In addition, two sFv clones (3R6-1 and 2R6-21) that mapped to the cyclin box domains markedly inhibited Tat-mediated transactivation in several transiently transfected cell lines without inhibiting basal transcription or inducing apoptosis. When HIV-1 challenge studies were performed on stable 3R6-1-expressing Jurkat T cells, near complete inhibition of viral replication was obtained at a low challenge dose, and 74–88% inhibition to HIV-1 replication was achieved at a high infection dose in SupT1 cells. These results provide proof-in-principle that anti-hCyclinT1 intrabodies can be designed to block HIV-1 replication without causing cellular toxicity, and as a result, they may be useful agents for “intracellular immunization”-based gene therapy strategies for HIV-1 infection/AIDS.

The HIV¹ transactivator protein Tat is absolutely required for viral replication. In the absence of Tat the transcription of

HIV mRNAs can be initiated but cannot be efficiently elongated to produce full-length viral RNA genome (1). Tat interacts specifically with human cyclinT1 (hCyclinT1), a regulatory partner of cyclin-dependent kinase 9 (Cdk9) in the positive transcription elongation factor (P-TEFb) complex. Tat binds cooperatively with hCyclinT1 to the transactivation response element (TAR), a bulged RNA loop structure located at the 5'-end of nascent viral RNA transcripts to recruit P-TEFb and promote HIV transcription elongation. The assembly of the Tat-TAR-P-TEFb complex to the HIV promoter activates the Cdk9 kinase activities, which further autophosphorylates P-TEFb and hyperphosphorylates the C-terminal domain of RNA polymerase II (2), leading to the formation of processive elongation complexes that synthesize full-length HIV viral mRNA. In addition to hCyclinT1 and Cdk9 subunits, the nascent P-TEFb complex also contains hCyclinT2a, T2b, (3) and recently described 7SK small nuclear RNAs as well as several other proteins of unknown identity (4, 5). Among these, only Cdk9/hCyclinT1 heterodimer functions as both a general and an HIV-1 Tat-specific transcription factor (2, 6, 7, 8).

The transactivation mechanism is a particularly attractive target for the development of new anti-retroviral drug therapies, because Tat is required for viral gene expression not only during the exponential growth of the virus, but also, critically, it is required during the activation of the integrated proviral genomes that give rise to drug-resistant strains of HIV-1 (9). With the recent advances in our understanding of the molecular mechanisms of transactivation, it is clear that one novel anti-retroviral strategy that would bypass the ability of HIV-1 to adapt to traditional anti-viral therapies is to develop agents that target hCyclinT1. This would be an attractive target, if it was possible to selectively disrupt Tat-hCyclinT1 interactions without disrupting the function of the P-TEFb complex, which is required for basal cellular transcription. Indeed, although hCyclinT1 contains 726 amino acids (see Fig. 1), the N-terminal 272 residues, including the entire cyclin domain (residues 1–250) and a TAR recognition motif (TRM, residues 250–272 of hCyclinT1) fully support the Tat transactivation of HIV-1 LTR (long terminal repeat) (10), whereas the C-terminal 300 amino acids (residues 402–701) are believed to mediate the coupling of general transcription elongation and pre-mRNA splicing (11).

In previous studies we have demonstrated that an intrabody to HIV-1 Tat could significantly inhibit HIV-1 replication *in*

* This work was supported by a National Research Service Award and Center for AIDS Research Development Award (to J. B.), by Grants 5R01-RR14447 and 2R01-AI28785 from the National Institutes of Health (to W. A. M.), and by a joint Dana-Farber Cancer Institute-Beth Israel Deaconess Medical Center and Children's Hospital Center for AIDS Research grant. W. Marasco has a financial interest in Abgenix. The costs of publication of this article were defrayed in part by the payment of page charges. This article must therefore be hereby marked “advertisement” in accordance with 18 U.S.C. Section 1734 solely to indicate this fact.

¶ To whom correspondence should be addressed: Dept. of Cancer Immunology and AIDS, Dana-Farber Cancer Institute, JFB# 824, 44 Binney St., Boston, MA 02115. Tel.: 617-632-2153; Fax: 617-632-3113; E-mail: Wayne_Marasco@DFCI.Harvard.Edu.

¹ The abbreviations used are: HIV, human immunodeficiency virus; hCyclinT1, human cyclinT1; Cdk9, cyclin-dependent kinase 9; P-TEFb,

positive transcription elongation factor complex; TAR, transactivation response element; TRM, Tat-TAR recognition motif; LTR, long terminal repeat; sFv, single-chain antibody; mAb, monoclonal antibody; HA, hemagglutinin; HRP, horseradish peroxidase; GST, glutathione S-transferase; PBS, phosphate-buffered saline; ELISA, enzyme-linked immunosorbent assay; CMV, cytomegalovirus; NLS, nuclear localization signal; NOL, nucleolar localization signal; snRNA, small nuclear RNA; TCID₅₀, 50% tissue culture infectious dose.

vitro (12, 13) indicating that the Tat transactivation pathway could be targeted by intrabodies specific for the viral component of this pathway. Based on these studies, we further hypothesized that, because the molecular interaction between HIV-1 Tat and the N-terminal region of hCyclinT1 is necessary for HIV-1 replication, the selective disruption of this binding by anti-hCyclinT1 intrabodies could inhibit Tat-mediated transactivation and HIV-1 replication without having a detrimental effect on basal transcription. To test this hypothesis, we used the N-terminal region of hCyclinT1 and a synthetic TRM peptide to screen a very large non-immune human single-chain antibody (sFv) phage display library to identify sFvs that could be engineered as anti-hCyclinT1 intrabodies. Of the five hCyclinT1-specific single chain antibody (sFv) clones that were identified, one sFv (3R6-1) not only disrupted the molecular interaction between Tat and hCyclinT1 in co-transfected human CD4⁺ T cell lines but also inhibited HIV-1 replication upon viral challenge. Importantly, no disruption of basal cellular transcription was observed. These results provide proof-in-principle that anti-hCyclinT1 intrabodies can be designed to selectively block Tat-mediated transactivation and HIV-1 replication. They may also provide a promising new agent for the gene therapy of HIV-1 infection.

EXPERIMENTAL PROCEDURES

Antibodies—Anti-M13 monoclonal antibody (mAb) were obtained from Amersham Biosciences. Goat anti-human cyclinT1, rabbit anti-human Cdk9, rabbit anti-HA, rabbit anti-His, and goat anti-HA IgG beads were purchased from Santa Cruz Biotechnology. Horseradish peroxidase (HRP)-conjugated goat anti-mouse IgG and HRP-conjugated mouse anti-goat IgG were purchased from Pierce (Rockford).

Construction of Expression Vectors—Prokaryotic expression vectors pGST-hT1-250 and pGST-hT1-300 for producing truncated hCyclinT1-GST fusion proteins were kindly provided by Dr. Peterlin (10). To express GST-full-length hCyclinT1 fusion protein, the hCyclinT1 gene amplified by PCR with built-in *Bam*HI and *Eco*RI sites was inserted into pGEX-2T (Amersham Biosciences), resulting in pGST-hT1-726. pGST-hT1-200 was created by digesting pGST-hT1-726 with *Eco*RI and *Bsm*I followed by blunt-end ligation to remove amino acids 202–726 in hCyclinT1 (see Fig. 3A). The eukaryotic expression vector for hCyclinT1 (pCI-86) was provided by Dr. Jones (8). pCI-86(His) vector for expressing C-terminally His-tagged hCyclinT1 was constructed by replacing the original C-terminal *Bst*BI/*Not*I fragment with a similar PCR-modified fragment containing sequence coding for six histidines.

For expressing soluble sFvs in bacterial cells, sFv coding sequences were isolated from the pFarber phage display vector by *Nco*I and *Not*I digestion and inserted into the pSyn1 vector in the same orientation. The sFvs expressed in bacterial cells were C-terminally tagged with c-myc and His₆ (Fig. 2A). For expressing sFv intrabodies in mammalian cells, the sFv coding sequences were released from pFarber phage display vectors by *Sfi*I and *Not*I digestion and ligated into an sFv expression cassette in psFv-Ck-HA (Fig. 5A).

Purification of Bacterially Expressed GST and sFv Fusion Proteins—GST fusion proteins were purified using glutathione-Sepharose 4B beads following the manufacturer's instructions (Amersham Biosciences). Single colonies of transformed XL1-blue bacteria were cultured at 37 °C overnight in 10 ml of 2xYT medium containing 100 µg/ml ampicillin. The overnight culture was used to inoculate 1 liter of fresh medium followed by shaking for 3–5 h until 0.3–0.5 A_{600 nm} was achieved. Subsequently, isopropyl-1-thio-β-D-galactopyranoside was added at 0.5 mM to induce the expression of GST fusion proteins at 30 °C with vigorous shaking for 3–5 h. The bacterial pellets were resuspended in 50 ml of cold PBS containing protease inhibitor cocktails (Roche Molecular Biochemicals) and sonicated for 3 min in an ice bath. After centrifugation, the clear protein supernatants were mixed with pre-washed glutathione-Sepharose beads for 30 min. The column bed was then washed in cold PBS, and GST fusion proteins were eluted with 10 mM reduced glutathione solution and stored at 4 °C for ELISA assay or immunoprecipitation. For the isolation of GST-free hCyclinT1-200, -250, and -300 polypeptides, 1 ml of thrombin/PBS was added to the Sepharose bed. Cleaved hCyclinT1 polypeptides were collected by draining the column and washing with PBS. Protein concentrations were determined by the Bio-Rad protein assay.

To purify His-tagged sFvs, bacterial cultures were processed as de-

scribed above. Supernatants of cell lysates were clarified through a syringe filter. Proteins from 1 liter of culture were precipitated in 50% saturated ammonium sulfate and dissolved in 10 ml of PBS buffer containing 10 mM imidazole before being loaded onto a nickel-bound chelating Sepharose column (Amersham Biosciences). After washing with 20–200 mM imidazole in PBS buffer, His tag-bound proteins were eluted with PBS containing 300 mM imidazole.

Screening of Human sFv-phagemid Library—Construction of the pFarber phagemid display vector and characterization of a 15-billion member non-immune human sFv phage display library will be described elsewhere.² Phage particles displaying human sFv molecules from TG1 *Escherichia coli* host cells by VCS M13 helper phage and concentrated by PEG/NaCl precipitation and diluted to 10^{12–13} plaque-forming units/ml before screening (14–16).

To identify sFv clones that specifically bind to epitopes in the N-terminal region of hCyclinT1 that are involved in Tat transactivation, the phage display library containing 10¹² plaque-forming units was panned against affinity-purified GST-free hCyclinT1-300-coated Maxisorb immunotubes (20 µg/ml, Nalge Nunc International (15, 16)) for three successive rounds. After extensive washing with 0.1% Tween-20/PBS, bound phages were eluted with 100 mM triethylamine for 30 and 60 min. Pooled samples were used for rescue and further panning. After the last round of selection, selected sFv phages were diluted and used to infect TG1 *E. coli* strain. Culture medium containing sFv phage particles rescued from individual colonies in 24-well plates were submitted for ELISA screening.

To identify TRM-specific sFvs, a biotin-labeled TRM peptide (NR-LKRIWNWRACEAAKKGGK-biotin) was synthesized for screening the library from 200 to 2 ng concentration. Peptide-bound phages were trapped by streptavidin Immunobeads and eluted with 0.1 M HCl-glycine (pH 2.2) for 30 and 60 min. Individual clones rescued from rounds 3–7 were further analyzed by ELISA screening.

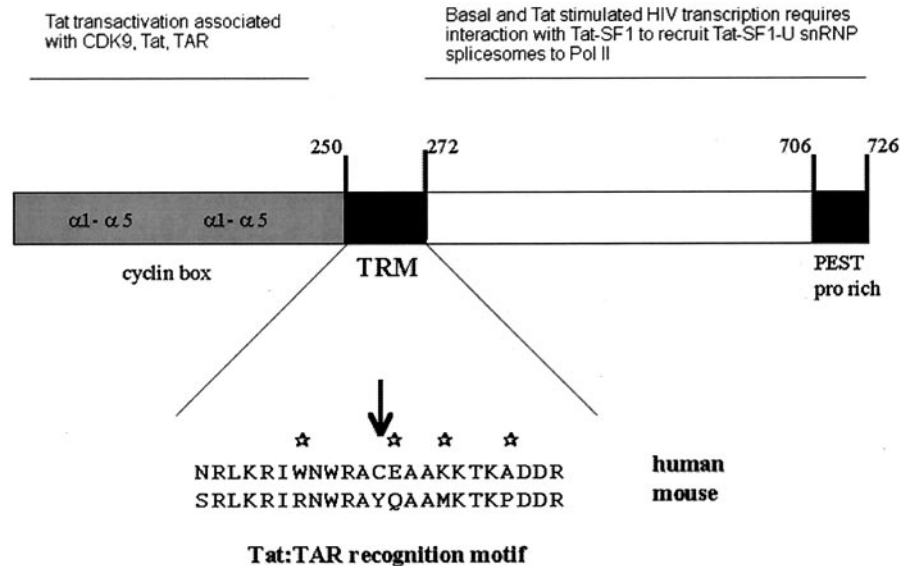
Phage ELISA—96-well microtiter plates were coated with purified GST-hCyclinT1-726 protein (10 µg/ml) followed by incubation with sFv phage particles (10¹⁰ plaque-forming units). The binding activity of anti-hCyclinT1 sFv phages to the antigens was determined by incubation with anti-M13 monoclonal antibodies and goat anti-mouse IgG-HRP. Positive samples were further tested with GST-coated plates to remove GST-specific sFv binders. VCS M13 helper phage stocks with a similar number of virus particles were used as negative control. sFv clones from peptide panning were screened on streptavidin-coated microtiter plates followed by incubation with biotin-TRM peptide and then with sFv phage particles. TRM-positive binders were further tested with purified hCyclinT1 as described above.

Real-time Biacore (Biospecific Interaction Analysis)—The binding affinity and kinetic profiles of isolated anti-hCyclinT1 sFvs to hCyclinT1 were analyzed by surface plasmon resonance on the Biacore 1000 apparatus (Amersham Biosciences). The flow cells of a CM5 sensor chip was tested under three different pH conditions. The GST-free hCyclinT1-300 could not be efficiently immobilized to the CM5 sensor chips under neutral (5 mM maleate, pH 6.0–7.0) or acidic pH conditions (10 mM acetate, pH 4.8); however, the sensor chips were effectively coupled with GST-hCyclinT1-300 (20 µg/ml) at pH 4.8 in the presence of 10 mM acetate. The level of immobilization was 24 ng of protein/mm² surface, equivalent to 24,000 relative units/mm² over background. Binding kinetic parameters for individual sFv clones were measured with His tag-purified sFv proteins at different concentrations. 2R6-21 and 3R6-1 were measured at 6.6, 33, 165, 330, and 660 nM, whereas 2R6-113 was measured at 330, 825, 1650, and 3300 nM. Association (*K*_{on}) and dissociation (*K*_{off}) constants of sFvs to hCyclinT1 were calculated with Biacore evaluation software based on simulated binding curves of actual measurements.

Establishment of sFv-intrabody Expressing Stable T Cell Transfectants—Human Jurkat and SupT1 cell lines (ARRRP-NIH) were cultured in RPMI 1640 growth medium supplemented with 10% fetal calf serum and 100 units of penicillin and streptomycin. To establish T cell transfectants that stably expressed anti-hCyclinT1 intrabodies for HIV-1 challenge, Jurkat and SupT1 cells were split 48 h prior to DNA transfection, washed in PBS, and then diluted to 3 × 10⁶ cells/ml in RPMI 1640 growth medium. The diluted cells (1 ml) were gently mixed with *Sca*I-linearized psFv-Ck-HA (8 µg) and transferred to a sterile chamber followed by electroporation. The transfected cells were cultured at 37 °C for 48 h to allow cells to recover, and, subsequently, the

² S. Mehta, Y. Wang, A. St. Clair Tallarico, and W. A. Marasco, manuscript in preparation.

FIG. 1. The molecular structure of the human cyclinT1 (hCyclinT1). The N-terminal 272 amino acids participate in the HIV-1 Tat-mediated transactivation. The C-terminal region is predicted to participate in basal and Tat-stimulated HIV transcription through interaction with Tat-SF1 and recruitment of Tat-SF1-U snRNP spliceosomes to RNA polymerase II (11). $\alpha 1$ - $\alpha 5$, α helix motifs; TRM, Tat-TAR recognition motif. The arrow-head indicates the point mutation of a key amino acid (C261Y) in mouse cyclin T1 that abolishes the molecular interaction between mouse cyclinT1 and HIV-1 Tat (10, 18). Asterisks highlight the sequence differences of the TRM motif between mouse and human cyclinT1 proteins.



cells were selected in growth medium containing G418 (1 mg/ml) for 3 weeks to derive G418-resistant cells.

HIV-1 Infection of T Lymphocytes—Bulk populations of stably transfected Jurkat and SupT cells in log phase of growth were harvested and washed in PBS. Subsequently, 5×10^5 cells were resuspended in 1 ml of growth medium containing 50 or 2500 TCID₅₀ infection units of HIV-1 III_B virus (17). After 2-h incubation at 37 °C, infected cells were washed in serum-free medium twice and were cultured in duplicate 6-well dishes for 3 weeks. Culture medium (1 ml) was collected at intervals of 2–3 days and frozen at –70 °C for p24 assay.

HIV p24 Antigen Assay—The concentration of HIV-1 core protein antigen in culture medium was measured by using a p24 immunoassay from Coulter Corp. (Westbrook, ME). The results were read on a Dynatech MR5000 enzyme-linked immunosorbent assay (ELISA) plate reader (Dynatech Laboratories Inc., Chantilly, VA). Medium samples were first tested without dilution. Samples that gave optical density readings of more than 1.0 were diluted at 1:10, 1:10², 1:10³, 1:10⁴, and 1:10⁵ and were re-assayed.

RESULTS

Identification of Human sFvs against hCyclinT1—To identify hCyclinT1-specific sFvs, the affinity-purified hCyclinT1 polypeptide (hCyclinT1–300) was used to coat immunotubes for screening the phage display library. The bait protein contained the N-terminal region 300 amino acids of hCyclinT1 that participates in Tat transactivation (Fig. 1). After three rounds of selection, individual colonies were tested by phage ELISA against purified GST-hCyclinT1–300 and GST. Approximately 80% colonies from the third round of panning were positive for hCyclinT1, and only 1 of 200 colonies reacted to GST. DNA sequence analysis of 50 binders positive for hCyclinT1 identified one unique sFv clone (3R6-1). To identify more diversified anti-hCyclinT1 sFv clones, phages from the second round of panning were used for ELISA screening. In addition to 3R6-1, two more sFv clones, 2R6-21 and 2R6-113, were identified. 3R6-1 and 2R6-21 clones predominated in the phage populations of the second round of selection, whereas 2R6-113 represented a small proportion (2%) of the positive binders.

The TRM motif of hCyclinT1 contains a cysteine residue (Cys-261) that has been shown to be critical for Tat and hCyclinT1 interaction (Fig. 1) (18). To identify TRM-specific sFvs, immunotubes were coated with the synthetic 20-mer peptide and one clone (PS11) was isolated after the second round of selection. When the same peptide was used for liquid phase selection with streptavidin beads, one additional sFv clone (S84) was isolated after seven rounds of panning. Table I shows the comparison of deduced amino acid sequences of the five

hCyclinT1-specific sFv clones. It is noteworthy that 3R6-1 and 2R6-21 share identical heavy chains, but have 13 amino acid differences in their light chains. These variations are mainly located in FW1 (PCR primer annealing region) and FW4 (different J λ segments) of V_L with one amino acid substitution in CDR2 and two substitutions in CDR3 that might account for their differential binding affinities *in vitro* and in mammalian cells described below. In addition, although PS11 and S84 were specific to the TRM motif, their amino acid sequences were very different.

Epitope Mapping of Anti-hCyclinT1 sFv Clones—To characterize the biochemical and binding properties of the anti-hCyclinT1 sFvs, the sFv coding sequences were subcloned into the pSyn1 bacterial expression vector to produce soluble 30-kDa sFv proteins that contain C-terminal c-myc followed by a His (x6) tag (Fig. 2A). Fig. 2B shows SDS-PAGE analysis of the sFv proteins purified from XL1-blue *E. coli* bacteria using nickel-chelating Sepharose columns. Purified GST fusion proteins containing different-length N-terminal hCyclinT1 amino acids or GST alone were used to coat microtiter plates to determine sFv binding epitopes on hCyclinT1 (Fig. 3A). To avoid nonspecific binding activity, the sFv concentrations used in these studies were first pre-determined by testing the serially diluted purified sFvs against a fixed amount of GST-free hCyclinT1–300, and then the sFvs were tested for binding at low concentrations above the end point of their binding activity (refer to Fig. 3C). As shown in Fig. 3B, the five sFvs bound specifically to GST-hCyclinT1 fusion proteins but not to GST. SFv 3R6-1, 2R6-21, and 2R6-113 bound strongly to GST-T1–200, GST-T1–250, and GST-T1–300, indicating that the epitopes for these sFvs were located within the cyclin box domains of the N-terminal 200 amino acids. Although the sFv 3R6-1 and 2R6-21 have identical V_H chains and closely related light chains, there was a 2-fold higher binding signal for 3R6-1 compared with 2R6-21 when tested at 0.05 μ g/ml sFv protein that reflects a difference in binding affinities for the two sFvs under these assay conditions. PS11 displayed stronger binding activity to GST-T1–300 than to GST-T1–250 as expected, because the TRM peptide used for panning corresponded to amino acids 250–266 of hCyclinT1. However, S84 showed only weak binding activity to GST-T1–300 and similarly cross-reacted with GST-T1–250 as well, indicating that a TRM-like epitope may be present in residues 200–250 of hCyclinT1.

Determination of sFv Binding Affinities to hCyclinT1—To

TABLE I
Heavy and light chain regions

The framework regions 1–4 and complementarily determining regions 1–3 for both the V_H and V_L genes are shown. The V_H and V_L family designations are 3R6-1, 2R6-21, and S84 = V_H^3 , V_L^6 ; PS11 = V_H^1 , V_L^1 .

Heavy chain variable region									
1	FW1	CDR1	FW2	CDR2	FW3	CDR3	FW4	121	
3R6-1	MAQVQLVQSGGGLVQPGSLRLSCAASGFTF	DDYAMHW	VRQAPGKGLEWV	SGISWNSGSIQYADSVKQ	RFITSRDNTKNTVTLQMNLSLRADTAIVYCVR	ALLDQWGGD	YWGQGTILVTVSS		
2R6-21	SSH.....	AV..YDGSNKY.....	DFGGVA..T..	Y.....		
S84	S..Y..S.	AT..KPDGNEKY..V.....	--MYGDAL..	K.....		
2R6-113	TS..GIS.	GW..AYNDNTH..QKQLQ.	--T..AAM.	V.....		
PS11		
Light chain variable region									
137	FW1	CDR1	FW2	CDR2	FW3	CDR3	FW4	242	
3R6-1	QSALTQPPSPASGTFPGQRTISC	SGSSSNIGS-NTVN	WYQQLPGTAPKLLIY	ANNQRES	GYPDRVSGS--RSGTSASLAISGLQSEDEADYYC	AAWDDSLNGAV	FGGTQLTLVL		
2R6-21	LPVM.....	R.....		
S84	T.....AGYD..H	G..N...		
2R6-113	NFM.....H.V..ES..KT...	T...GS..A..NY..H	ED.....	QSY...--MDNP.		
PS11	SYE.....D....		

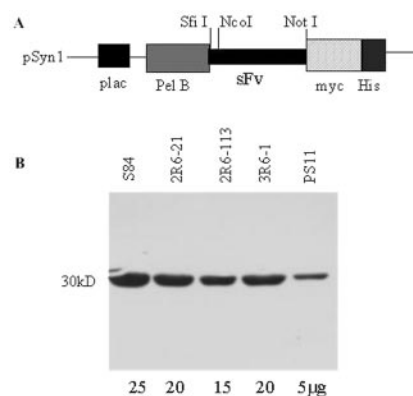


FIG. 2. Purification of anti-hCyclinT1 sFv proteins from bacterial cells. A, prokaryotic expression vector pSyn1. SFv inserts were isolated from the pFarber phage display vectors by *NcoI* and *NotI* digestion and ligated into pSyn1 vectors cleaved with the same restriction enzymes. SFv proteins expressed from transformed XL-1 Blue were C-terminally tagged with Myc and six histidines to facilitate affinity purification on nickel-bound chelating Sepharose column as described under "Experimental Procedures." B, His tag-purified 30-kDa anti-hCyclinT1 sFvs were analyzed in a 10% SDS-PAGE gel and stained with Coomassie Brilliant Blue. The amounts of each protein sample loaded are indicated.

further characterize the binding profiles of the anti-hCyclinT1 sFvs, microtiter plates were coated with purified GST-free hCyclinT1–300 (20 μ g/ml, equivalent to 660 nM), and the purified sFvs were tested for binding activity over the 0.033–1320 nM range (equivalent to 0.001–40 μ g/ml). As shown in Fig. 3C, the 2R6-21 and 3R6-1 clones yielded the strongest binding activities to purified hCyclinT1 with detectable binding at concentrations as low as 0.16 nM. Clones 2R6-113 and PS11 had similar binding profiles, however, their binding end points to hCyclinT1 were about 3.33 nM and were much higher than those seen for clones 2R6-21 and 3R6-1. Clone S84 had the lowest end point binding activity (82.5 nM) to the purified hCyclinT1. In addition, only the binding of sFv S84 and PS11, but not sFv 3R6-1, 2R6-21, or 2R6-113, to hCyclinT1–300 could be specifically blocked by the TRM peptide used for their selection in an ELISA-based peptide-blocking assay. As expected, a higher concentration of TRM peptide was required to compete for sFv PS11 compared with sFv S84 binding, which is most likely due to the relatively higher binding affinity of sFv PS11 to hCyclinT1–300 (data not shown).

To more accurately characterize the binding affinities of these sFvs to hCyclinT1, real-time Biacore analysis was performed and the association (K_{on}) and dissociation (K_{off}) constants for anti-hCyclinT1 sFv binding to hCyclinT1–300 were experimentally determined. Table II summarizes the results for the real-time Biacore analyses. The binding affinity of sFv 2R6-21 ($K_D = 6.95 \times 10^{-8}$ M) was 1.5-fold higher than 3R6-1 ($K_D = 1.07 \times 10^{-7}$ M) and 11-fold higher than 2R6-113 ($K_D = 7.94 \times 10^{-7}$ M). Because 2R6-21 and 3R6-1 share identical heavy chains, this result is consistent with the known finding that the majority of binding energy is often supplied by V_H CDR3 and different V_L chains can variably contribute to the overall energy of binding. Although S84 gave rise to positive binding signals at 82.5–660 nM concentrations in ELISA (Fig. 3C), it only showed background binding to hCyclinT1 in the Biacore assay even at much higher concentrations (330–3300 nM, data not shown), indicating that the Biacore assay had lower sensitivity than the ELISA assay. The binding parameters for PS11 were not measured using Biacore, however, the ELISA binding profile for PS11 is similar to that for sFv 2R6-113, suggesting that these two sFvs have similar binding affinities. Taken together, the binding affinity rank for these five

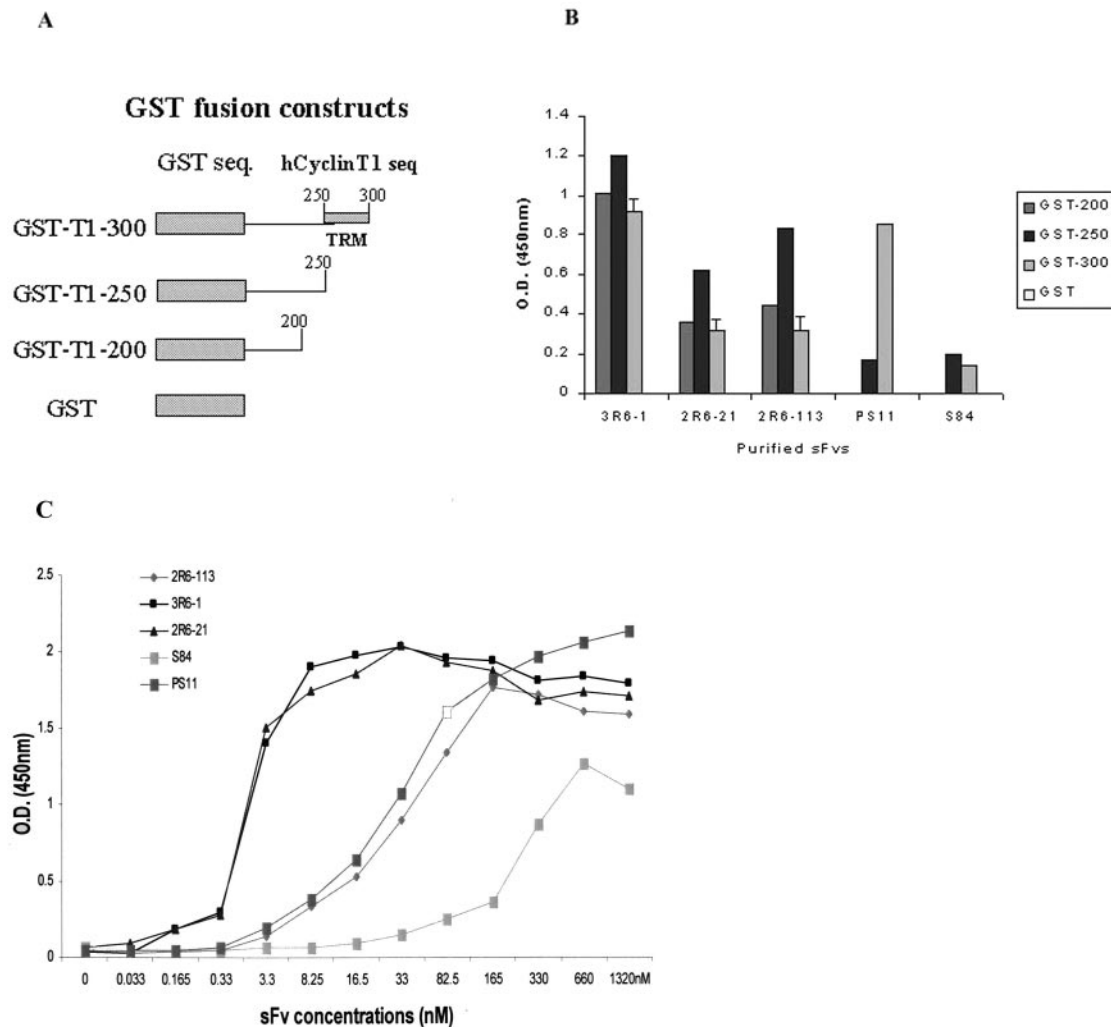


FIG. 3. **Epitope mapping of anti-hCyclinT1 sFvs.** A, prokaryotic expression constructs used for producing GST-hCyclinT1 fusion proteins that contained 200, 250, and 300 amino acids of the hCyclinT1 N-terminal region. GST and GST fusion proteins were purified using a glutathione-Sepharose 4B column. B, epitope mapping by ELISA. Microtiter plates were coated with 10 $\mu\text{g}/\text{ml}$ GST and GST-hT1 fusion proteins overnight at pH 9.0. Duplicate wells were incubated for 1 h at room temperature with varying concentrations of purified His-tagged sFvs followed by incubation with rabbit anti-His antibody (1:500) as primary antibody and horseradish peroxidase (HRP)-labeled goat anti-rabbit IgG (1:25,000) as secondary antibody. The optimal concentrations of sFvs used in this assay were pre-determined and chosen to be above their lowest detectable level of binding (end point binding activity) to avoid nonspecific reactions that could occur due to the use of high concentrations of sFv proteins. 3R6-1 and 2R6-21: 0.05 $\mu\text{g}/\text{ml}$; 2R6-113 and PS11: 0.5 $\mu\text{g}/\text{ml}$; S84: 5 $\mu\text{g}/\text{ml}$. C, determination of binding properties for anti-hCyclinT1 sFvs. Microtiter plates were coated with purified GST-free hCyclinT1-300 polypeptide (20 $\mu\text{g}/\text{ml}$) overnight. Binding of the different concentrations of purified His-tagged sFvs (0.033–1320 nM) to the plates was determined.

anti-hCyclinT1 sFvs was determined to be 2R6-21 > 3R6-1 > 2R6-113 \approx PS11 \gg S84.

Purified Anti-hCyclinT1 sFvs Could Precipitate Human CyclinT1-GST Fusion Proteins—To demonstrate whether purified anti-hCyclinT1 sFvs could bind to soluble hCyclinT1, an immunoprecipitation assay was conducted with purified His-tagged sFvs and GST-hT1-300 fusion proteins. The sFv-hCyclinT1 complexes were co-immunoprecipitated by anti-His mAb-conjugated microbeads. As shown in Fig. 4, sFv 3R6-1, 2R6-21, and 2R6-113 effectively bound to soluble GST-hT1-300. Compared with these sFvs, S84 showed less efficiency in co-immunoprecipitation, which is consistent with its lower binding affinity to hCyclinT1.

Anti-hCyclinT1 sFv Intrabodies Expressed in Mammalian Cells Bind to hCyclinT1—It has been previously reported that the addition of a human immunoglobulin kappa chain constant region to an anti-HIV-1 Tat sFv significantly increases the ability of the anti-Tat intrabody to inhibit Tat-mediated transactivation and HIV-1 replication, presumably by improving intracellular folding and increasing binding affinity due to

TABLE II
Affinity binding constants for anti-hCyclin T1 sFVs as determined by Biacore analysis

SFv	K_{on} $M^{-1} s^{-1}$	K_A M^{-1}	K_{off} s^{-1}	K_D M
2R6-113	2.38×10^3	1.26×10^6	1.89×10^{-3}	7.94×10^{-7}
2R6-21	1.96×10^4	1.44×10^7	1.36×10^{-3}	6.95×10^{-8}
3R6-1	1.3×10^4	9.38×10^6	1.38×10^{-3}	1.07×10^{-7}

dimerization (12). Therefore, to characterize the biological functions of anti-hCyclinT1 intrabodies in mammalian cells, the sFv coding sequences were subcloned into a pcDNA-based expression vector that directs the cytoplasmic expression of sFv-C κ -HA fusion proteins from the CMV promoter (Fig. 5A). As shown in Fig. 5B, the ~ 43 -kDa anti-hCyclinT1 sFv-C κ -HA-tagged fusion proteins were all expressed at comparable levels in transfected 293T cells except for PS11, which was expressed at a lower level.

To determine whether the anti-hCyclinT1 sFv-C κ -HA intra-

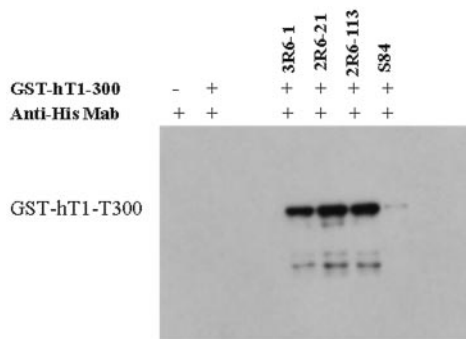


FIG. 4. Immunoprecipitation of human cyclinT1 by purified anti-hCyclinT1 sFvs. GST-hT1-300 (20 μ g) was incubated with each His-tagged sFv (5 μ g) in 500 μ l of binding buffer (PBS supplemented with 0.1% bovine serum albumin and 0.5 M NaCl) for 2 h at room temperature followed by incubation overnight at 4 °C with 20 μ l of microbeads containing 40 μ g of anti-His mAbs. The microbeads were pre-blocked with 5% milk/binding buffer for 1 h at room temperature before being added to the binding reaction. After serial washes, sFv/GST-hT1-300 immune complexes pulled down by anti-His mAb-conjugated microbeads were analyzed on 10% SDS-PAGE followed by detection for precipitated GST-hT1-300 by Western blot using HRP-conjugated mouse anti-GST mAbs.

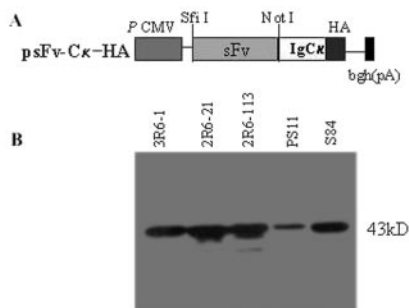


FIG. 5. The expression of anti-hCyclinT1 intrabodies in mammalian cells. A, eukaryotic vectors (psFv-Ck-HA) for expressing anti-hCyclinT1 intrabodies. SfiI inserts from the pFarber phage display vector were isolated by SfiI and NotI digestion and ligated into the vector to create sFvs that are fused to the human Ig κ chain constant region to increase intracellular folding and binding affinity (23). B, anti-hCyclinT1 intrabody expression vectors were transfected into 293T cells by using Qiagen Polyfect reagent and 24 h post-transfection, cells were lysed with 1 ml of lysis buffer (20 mM Hepes, pH 7.9, 0.5 M NaCl, 1% Nonidet P-40, 5 mM EDTA, 1 mM dithiothreitol, and 1 mM phenylmethylsulfonyl fluoride). The cell lysates (20 μ l) were analyzed on 10% SDS-PAGE followed by Western blot with rabbit anti-HA primary antibody and HRP-conjugated goat anti-rabbit IgG secondary antibody. The sFv fusion proteins are ~43 kDa.

bodies expressed in mammalian cells could bind to nascent cellular hCyclinT1, co-transfection and co-immunoprecipitation experiments were performed. An irrelevant sFv-Ck-HA intrabody (A3H5) served as a negative control. A full-length hCyclinT1-726 expression vector was modified to produce a C-terminal His-tagged hCyclinT1 protein (hCyclinT1-His) for these studies (8). Fig. 6A shows that all five anti-hCyclinT1 intrabodies and the A3H5 negative control were expressed at similar levels in transfected 293T cells, although PS11 is again expressed at lower levels. In addition, the hCyclinT1-His expression levels in the total cell lysates among the co-transfected 293T cells were very similar. As shown in Fig. 6B, the anti-hCyclinT1 sFv-Ck-HA intrabodies were also co-precipitated by goat anti-His IgG-conjugated agarose beads (Santa Cruz Biotechnology, Santa Cruz, CA) under conditions in which about 98% of the hCyclinT1-His was precipitated (data not shown). hCyclinT1 heterodimerizes with its partner Cdk9 to form the P-TEFb complex, which is associated with the 7SK snRNA (4). The precipitated immune complexes also contained Cdk9 mol-

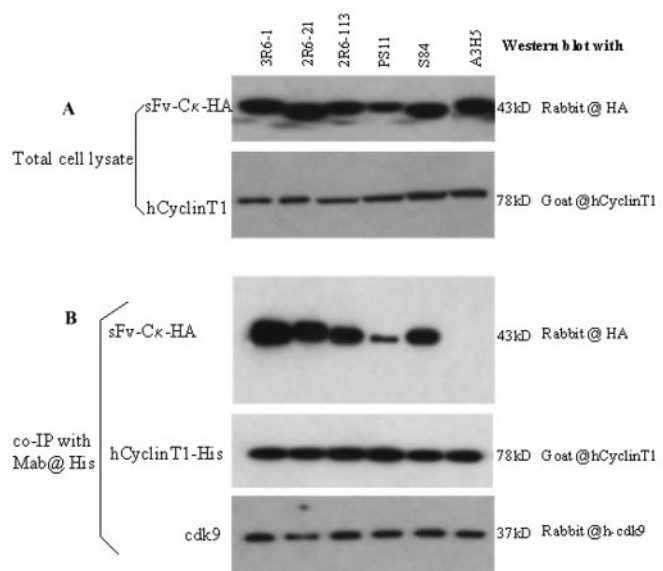


FIG. 6. Co-immunoprecipitation of nascent human cyclinT1 by anti-hCyclinT1 intrabodies expressed in mammalian cells. 293T cells were seeded overnight prior to DNA transfection. Each psFv-Ck-HA construct (4 μ g) and an equal amount of pCI-86(His) that directed the expression of C-terminally His-tagged human cyclinT1 were co-transfected into 293T cells in 10-cm dishes by Polyfect reagent (Qiagen). 24 h post-transfection, total cell lysate was made with 1 ml of lysis buffer in the presence of protease inhibitors. A, detection of anti-hCyclinT1 intrabodies and human cyclinT1 co-expressed in co-transfected 293T cells. Total cell lysates (20 μ l) from each transfection were analyzed by Western blot. Rabbit anti-HA primary antibodies and HRP-labeled goat anti-rabbit IgG secondary antibody were used to detect sFv-Ck-HA intrabodies and goat anti-His primary antibodies, and HRP-labeled mouse anti-goat IgG mAbs were used to detect human cyclinT1 proteins, respectively. B, co-immunoprecipitation of human cyclinT1-His and anti-hCyclinT1 intrabodies with anti-His mAbs. Cell lysate (200 μ l) was mixed with 30 μ l of mouse anti-His IgG-conjugated agarose beads that were pre-blocked with 2% milk/lysis buffer for 30 min on a rocking platform, and the mixtures were rocked overnight at 4 °C followed by three washes with the lysis buffer and two washes with PBS. The beads were then resuspended into 60 μ l of 1 \times protein loading buffer containing 100 mM dithiothreitol, boiled for 5 min, and analyzed on 10% SDS-PAGE followed by Western blotting for co-immunoprecipitation of hCyclinT1, sFv-Ck-HA, and Cdk9 with different antibodies against hCyclinT1 and sFv-Ck-HA as described in A. The human Cdk9 was detected by rabbit anti-human Cdk9 primary antibody and HRP-labeled goat anti-rabbit secondary antibody.

ecules, indicating that the P-TEFb complex was present and, importantly, that the anti-hCyclinT1 intrabodies did not disrupt the heterodimerization between hCyclinT1 and Cdk9. Also shown in Fig. 6B is that different amounts of anti-hCyclinT1 intrabodies were bound to co-expressed hCyclinT1-His and that the negative control sFv A3H5 showed no interactions with hCyclinT1-His, indicating that the co-immunoprecipitation was specific. Based on the signal intensities of the bound anti-hCyclinT1 intrabodies to hCyclinT1-His, the *in vivo* binding affinities of these anti-hCyclinT1 sFvs ranked 3R6-1 > 2R6-21 > 2R6-113 \approx S84 > PS11. For reasons that are not clear, in co-immunoprecipitation studies with anti-HA antibodies we were unable to effectively pull down the cellular components of the p-TEFb complex (data not shown).

Inhibition of Tat-mediated Transactivation by Anti-hCyclinT1 Intrabodies—The anti-hCyclinT1 intrabodies were next co-transfected into HIV-1-susceptible T cells with the HIV-1 Tat reporter gene system (pSV-tat and pHIV-1 LTR-luc) to evaluate their ability to inhibit Tat-mediated transactivation. A β -galactosidase expression vector driven by the SV40 promoter was used for normalizing the transfection efficiency. Only the three of the anti-hCyclinT1 intrabodies with the strongest *in vivo* binding affinities had inhibitory activity.

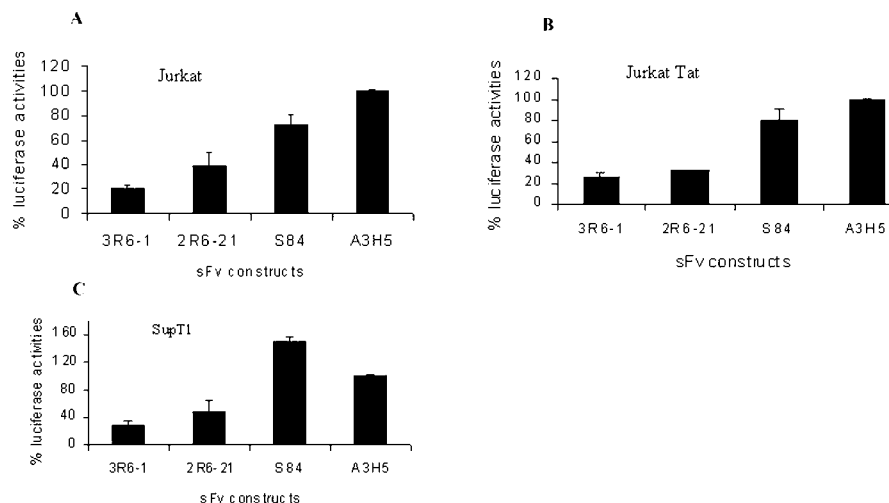


FIG. 7. Inhibition of HIV-1 Tat-mediated transactivation in human T cell lines by anti-hCyclinT1 intrabodies. Human Jurkat T cells (A) and SupT1 T cells (B) were transiently co-transfected with three anti-hCyclinT1 psFv-C κ -HA intrabody constructs (3R6-1, 2R6-21, and S84, 5 μ g each) together with pSV-tat (25 ng) and pHIV-1-LTR-luc (25 ng) by using Qiagen SuperFect reagent. HIV-1 Tat expressed from pSV-tat vector transactivated the reporter gene luciferase expression through HIV-1 LTR. A pSV- β -gal vector (1 μ g) was included in each transfection experiment to normalize the transfection efficiency. The irrelevant sFv A3H5 was used as a negative control. 24 h post-transfection cell lysate was made with 1 ml of cell culture lysis buffer and 50 μ l of lysate was used to perform a luciferase assay according to the manufacturer's instruction (Promega). The luciferase activity for the negative control sFv A3H5 construct was set to 100%, and the percentage of luciferase activities for each anti-hCyclinT1 intrabody construct was calculated accordingly. C, the transfection was conducted similarly except that Jurkat Tat cells stably express HIV-1 Tat proteins (19), therefore, the pSV-tat vector was omitted.

When compared with the irrelevant negative control A3H5, the sFv 3R6-1 and 2R6-21 intrabodies showed 80 and 60% reduction in Tat-mediated transactivation in Jurkat T cells, whereas sFv S84 displayed only 28% inhibition (Fig. 7A). In SupT1 cells, 3R6-1 and 2R6-21 showed 71 and 52% inhibition of transactivation but transactivation was increased with S84 compared with the A3H5 control (Fig. 7B). Stable Jurkat-Tat cells were also co-transfected with the anti-hCyclinT1 sFvs and pHIV-1 LTR-luc (19). As shown in Fig. 7C, the anti-hCyclinT1 intrabodies 3R6-1, 2R6-21, and S84 yielded 73, 67, and 20% reduction in Tat transactivation compared with the A3H5 control, a result consistent with the results obtained with Jurkat and SupT1 cells (Fig. 7, B and C). The anti-hCyclinT1 intrabodies 2R6-113 and PS11 showed no significant inhibition to Tat activation with any of the three cell lines tested (data not shown).

Anti-hCyclinT1 Intrabodies Expressed in Human T Cell Lines Suppress T-tropic HIV-1 Replication—To evaluate whether the anti-hCyclinT1 intrabodies could inhibit HIV-1 replication in HIV-1-susceptible T cells, the intrabody expression vectors were stably transfected into Jurkat and SupT1 T cell lines. The expression of anti-hCyclinT1 sFv-C κ -HA intrabodies 3R6-1, 2R6-21, and S84 as well as the negative control A3H5 showed no toxic effects on Jurkat- and SupT1-stable transfectants (data not shown). The bulk populations of stable Jurkat transfectants were infected with HIV-1_{IIIB} (50 units of TCID₅₀ per million cells) and cultured for 3 weeks. The control A3H5 and S84 transfectants showed extensive large syncytia formation on days 14–19 post-infection. The 2R6-21 transfectants also displayed syncytia formation but to a lesser extent, indicating that anti-hCyclinT1 2R6-21 and S84 did not protect infected Jurkat cells from cytopathic effects. The absence of inhibition of HIV-1 replication was not caused by the loss of 2R6-21 or S84 intrabody expression based on Western blot analysis (data not shown). In contrast, 3R6-1 transfectants showed no syncytia formation and were morphologically normal during the 21-day challenge period (data not shown). The results of p24 antigen assays for the HIV-1 challenge experiments with 3R6-1 and control A3H5 are shown in Fig. 8A.

Virus production from A3H5 transfectants was detected first on day 8 post-infection (182 pg/ml) and rapidly reached to the peak level of 347 ng/ml on day 21 post-infection. However, the viral replication in 3R6-1 transfectants was significantly inhibited and was below a detectable level on day 11. Subsequently, the viral replication remained markedly inhibited on day 21 post-infection (11 ng/ml, p24), the latest day post-infection that was examined, which represented ~97% reduction in the viral production compared with A3H5 control cells. When 3R6-1, 2R6-21, S84, or A3H5 control transfectants were infected with a 50-fold higher dose of HIV-1_{IIIB} (2500 TCID₅₀ per million cells), massive syncytia formation, severe cytopathic effects, and cell death were seen on day 7 post-infection indicating that the infection doses were too high to identify any differences in viral infection between the 3R6-1 and other anti-hCyclinT1 and control intrabody-expressing transfectants.

HIV-1 Tat protein is initially expressed in the cytoplasm of infected cells from spliced HIV-1 tat mRNA and subsequently translocated into the nuclei and nucleoli where it interacts with P-TEFb to increase the efficiency of elongation of full-length HIV-1 genomic RNA. Because this interaction occurs in nuclei and nucleoli of infected cells, nuclear and nucleolar targeting vectors were constructed to evaluate whether expression of the anti-hCyclinT1 intrabodies in the cytoplasm or in the nuclear or nucleolar compartments would give rise to stronger inhibition of HIV-1 replication.

Stable SupT1 transfectants that expressed anti-hCyclinT1 3R6-1 and control A3H5 intrabodies containing the SV40 nuclear localization signal (NLS) or the HIV-1 Tat nucleolar localization signal (NOL) (20) were additionally established and then infected with a high concentration of HIV-1_{IIIB} (2500 units of TCID₅₀ per million cells). Marked syncytia formations were seen with all SupT1 cells that expressed control intrabodies (A3H5, A3H5-NLS, and A3H5-NOL) beginning day 3 post-infection. As the viral replication progressed, cytopathic effects became more extensive and ballooning fused cells that contained hundreds of nuclei were seen on day 11 post-infection. In contrast, the cytopathic effects of HIV-1_{IIIB} on infected SupT1 cells that expressed the anti-hCyclinT1 intrabody 3R6-1 and its

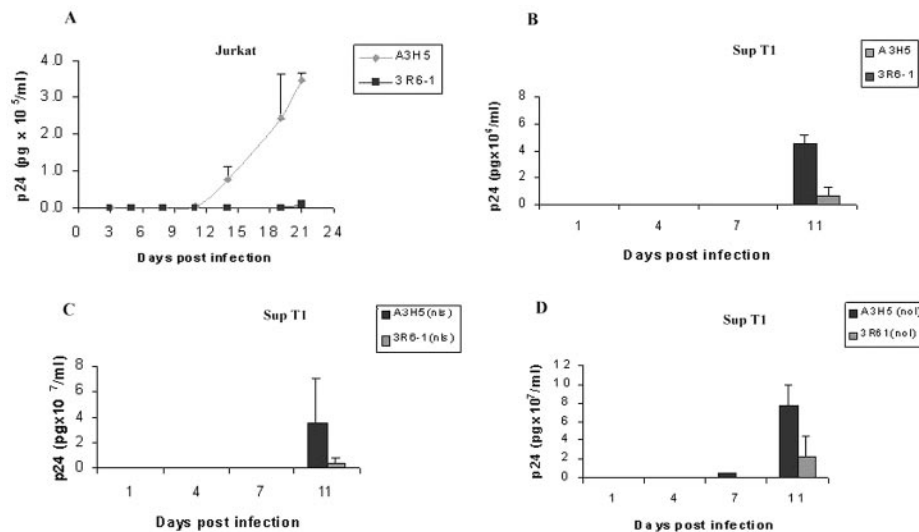


FIG. 8. *In vitro* HIV-1 challenge of Jurkat and SupT1 cells stably expressing anti-hCyclinT1 intrabodies. Jurkat or SupT1 transfectants were split 48 h before challenge. Cells were washed in PBS and resuspended into 1 ml of viral dilution medium containing T-tropic HIV-1 B_{III} virus and incubated at 37 °C for 2 h. Subsequently, the cells were washed and resuspended into 6 ml of growth medium supplemented with 10% fetal calf serum and 100 units of penicillin and streptomycin. Each set of infected cells was cultured in two wells in six-well plates. The medium was harvested at intervals of 2–3 days and stored at –70 °C for p24 assays. The infected cells were split simultaneously by 1:2 dilution. In A, Jurkat T cells were infected with HIV-1 III_B at 50 units of TCID₅₀. In B–D, SupT1 cells were infected with 2500 units of TCID₅₀. A3H5, negative control intrabody; 3R6-1, anti-hCyclinT1 intrabody. nls (sFv-C κ -NLS-HA) and nol (sFv-C κ -NOL-HA) represent intrabodies containing nuclear localization and nucleolar localization signals, respectively.

NLS or NOL derivatives were much less severe. For these cells, the onset of syncytia formation was delayed until day 6 post-infection, and only small syncytium formation was observed in 3R6-1-expressing cells, whereas SupT1 3R6-1-NLS cells showed no syncytial formation and SupT1 3R6-1-NOL cells displayed only rare small fused cells. These results indicated that the expression of anti-hCyclinT1 intrabodies 3R6-1 and its NLS- or NOL-containing derivatives significantly decreased the cytopathic effects of HIV-1 B_{III} on infected SupT1 cells (data not shown).

During the initial 4-day period post-infection, the p24 levels in the culture medium showed no significant differences between SupT1 cells that expressed different versions of A3H5 control and 3R6-1 intrabodies. However, p24 production in SupT1 cells that expressed anti-hCyclinT1 intrabodies 3R6-1 and its NLS and NOL derivatives were significantly reduced compared with their A3H5 counterparts (Fig. 8, B–D). On day 11 post-infection the viral replication in A3H5 transfectants progressed very rapidly and produced 4,545 ng/ml p24 antigen. Compared with this, the viral production in 3R6-1 transfectants was only 646 ng/ml, representing an 86% reduction in the viral replication at the same time point (Fig. 8B). For the SupT1 cells expressing NLS-containing intrabodies (Fig. 8C), the p24 production in 3R6-1-NLS transfectants on day 11 post-infection was 4,337 ng/ml, which represented only 12% of viral production in A3H5-NLS control (35,080 ng/ml). As for SupT1 cells that expressed NOL derivatives (Fig. 8D), on day 7 post-infection the viral replication was well controlled in the 3R6-1 transfectants and yielded 11 ng/ml p24 antigen, representing 0.2% of the viral production in control cells (4,464 ng/ml). On day 11 post-infection, compared with A3H5-NOL-expressing cells (77,640 ng/ml), the peak p24 levels in 3R6-1-NOL cell supernatants (22,200 ng/ml) was reduced about 71%. Interestingly, a cross comparison between SupT1 cells expressing 3R6-1 and its NLS or NOL derivatives showed that SupT1 transfectants that expressed 3R6-1-NLS and -NOL intrabodies displayed much less severe cytopathic effects compared with 3R6-1 transfectants. These results demonstrate that the anti-hCyclinT1 intrabody 3R6-1 is a potent agent that can signifi-

cantly reduce HIV-1 cytopathic effects and dramatically suppress HIV-1 replication *in vitro*.

DISCUSSION

The cytopathic effects of HIV-1 on CD4⁺ T lymphocytes cause rapid and continuous destruction of CD4⁺ T helper cells and lead to chronic, persistent infection and immune deficiency (21–23). The molecular interaction between HIV-1 Tat protein and hCyclinT1 in the P-TEFb complex is one of the most important pathways that regulates HIV-1 replication. The presence of proviruses in resting CD4⁺ T lymphocytes and the persistent release of infectious viral particles by activation of these latently infected cells results in a life-long, latent viral infection. Several investigators have demonstrated that the Tat-mediated transactivation pathway can be disrupted by genetic “intracellular immunization”-based strategies using anti-Tat intrabodies (24), antisense RNA and ribozyme-based genetic inactivation (25), anti-tat/rev interference RNA (26), and others (27). A major limitation of these approaches is the sequence variations in the HIV-1 Tat proteins or *tat* gene among the different virus isolates (28).

hCyclinT1 is a conserved cellular protein that is absolutely necessary for HIV-1 Tat-mediated transactivation and HIV-1 replication but is also a critical component of the cellular P-TEFb complex that is required for normal cellular transcription elongation. Therefore, the identification of human anti-hCyclinT1 intrabodies that specifically disrupt the molecular interaction between Tat and hCyclinT1 but do not interfere with its normal cellular function would be an ideal agent for HIV-1 gene therapy against diverse viral isolates. Toward this end, we employed a purified hCyclinT1–300 polypeptide containing the N-terminal region of hCyclinT1 as bait for screening a human phage display library and identified five distinct anti-hCyclinT1 sFvs. Three of these sFvs bound to the cyclin box domains and two sFvs mapped to the TRM motif. The hCyclinT1 N-terminal region, including the cyclin domains and TRM motif, fully supports HIV-1 Tat-mediated transactivation. Co-immunoprecipitation studies demonstrated that all of these anti-hCyclinT1 intrabodies specifically bound to co-expressed

hCyclinT1 in 293T cells. SFv clones 3R6-1 and 2R6-21 that bound to the cyclin box domain inhibited HIV-1 Tat-mediated transactivation in co-transfected Jurkat and SupT1 cells without significant effects on cellular function based on β -galactosidase activity. The expression of these sFvs did not promote apoptosis of Jurkat and SupT1-stable transfectants and did not disrupt hCyclinT1-Cdk9 interaction indicating that the P-TEFb functions were not affected. Upon HIV-1 challenge of stably transfected Jurkat and SupT1 cells, the 3R6-1 intrabodies that displayed the highest binding affinity to nascent hCyclinT1 not only significantly reduced the cytopathic effects of HIV-1 B_{III} but also markedly suppressed viral replication in infected Jurkat T cells at a lower challenge dose and achieved 71–88% inhibition to HIV-1 replication even at higher infection doses in SupT1 cells. These results provide a proof of concept that targeting Tat-hCyclinT1 interaction by anti-hCyclinT1 intrabodies is an effective approach for HIV-1 gene therapy that specifically disrupts the molecular interaction between HIV-1 Tat and hCyclinT1.

SFv clones 2R6-21 and 3R6-1 share the same V_H but have different V_L chains. Their binding epitopes were mapped to the cyclin box domains; however, it is not clear whether the two sFvs bind to the same epitopes. The *in vivo* binding activity of the 2R6-21 intrabody to the nascent hCyclinT1 was only slightly weaker than 3R6-1; however, sFv 2R6-21 did not inhibit HIV-1 replication upon challenge in Jurkat T cells, although it did significantly suppress Tat-mediated transactivation in transfected Jurkat, Jurkat-Tat, and SupT1 cells. It remains to be determined whether this lack of inhibition of HIV-1 replication for sFv 2R6-21 is caused by its lower *in vivo* binding affinity or its binding to a different epitope on hCyclinT1. It will be very interesting in future studies to determine the exact binding sites for these sFvs to hCyclinT1. This may shed further light on the one or more mechanisms by which these two intrabodies differentially block Tat-mediated transactivation and HIV-1 replication.

The TRM motif lies at the extreme C terminus of the cyclin domain (residues 250–265) and contains multiple residues that are critical to the binding of the hCyclinT1-Tat complex to TAR RNA (18). The TRM motif makes independent contact with Tat and TAR RNA, especially residues 259 (arginine) and 261 (cysteine) that are important for hCyclinT1-Tat interaction, which requires Zn²⁺ ions. In the current study, efforts were made to identify TRM-specific sFvs using the purified TRM-containing hCyclinT1–300 polypeptide for screening the phage display library. Three sFv clones were found that bound specifically for the cyclin box domains. However, no binders for the TRM were identified suggesting that the TRM may be masked by neighboring residues in the hCyclinT1–300 polypeptide that might prevent phage sFvs from binding, even though this region has a predicted high hydrophilicity index suggesting that it should be exposed to the aqueous phase. To overcome this problem, we used a biotinylated 20-amino acid polypeptide that contains the major part of the TRM (amino acids 250–266) to screen the sFv-phage library and identified two TRM-specific sFv clones. SFv S84 was identified using streptavidin beads to capture the polypeptide-bound phage. This sFv had very low binding affinity to denatured hCyclinT1–300 in the ELISA assay, showed good binding activity to the nascent hCyclinT1, and yielded mild inhibition to the HIV-1 Tat-mediated transactivation in Jurkat and Jurkat-Tat T cells but did not inhibit HIV-1 replication upon challenge. This may be due to its low binding affinity to endogenous hCyclinT1. The other clone, PS11, was identified using TRM peptide-coated immunotubes, and this sFv had a much higher binding affinity to denatured hCyclinT1–300 than S84, however, it only had weak binding

activity to nascent hCyclinT1 and showed no inhibition to Tat transactivation. Although the one or more reasons for lack of a significant inhibitory effect of these two TRM-specific sFvs on Tat-mediated transactivation or HIV-1 replication are not clear, it has been previously demonstrated that synthetic TRM peptides failed to form a specific complex with Tat and TAR, as did other fragments of hCyclinT1 lacking small regions of the cyclin box domain (18). These results suggest that maintenance of the natural conformation of the TRM in hCyclinT1 is necessary for Tat-TAR recognition by hCyclinT1 and this may also be important for isolating high affinity TRM-specific sFvs. Strategies that will allow us to better expose the TRM motif in hCyclinT1 and to simultaneously maintain its natural conformation will be important in future attempts to obtain high affinity human sFvs to completely epitope map that surface of hCyclinT1. These anti-hCyclinT1 sFvs can then be used for *in vitro* biochemical studies and *in vivo* animal studies to better understand how to more efficiently inhibit Tat transactivation and HIV-1 replication.

A priority for anti-HIV-1 gene therapy using intracellular immunization-based strategies is to reconstruct the defective immune system with cells that will be genetically resistant to HIV-1 infection and/or replication. Infusion of transduced autologous CD4⁺ T-cells expressing anti-HIV-1 resistance genes is the most immediate way to demonstrate proof-in-principle that the transduced cells have a survival advantage *in vivo* in HIV-1-infected individuals. However, pluripotent hematopoietic CD34⁺ stem cells are the best choice for the delivery of therapeutic constructs into humans long term, because these cells are self-renewing and can differentiate into multiple lineages of hematopoietic phenotypes, including HIV-1 targets T lymphocytes, macrophages, and dendritic cells that will aid in reconstituting severely damaged hematopoietic compartments. In addition, transduced CD34⁺ stem cells can provide sustained transgene expression *in vivo* for prolonged periods of time (29). The SCID-hu mouse model has been recognized as a unique *in vivo* system (30) to investigate HIV-1 pathogenesis (31, 32) and latent infection (33, 34) and is useful for the pre-clinical evaluation of the biological effects of anti-HIV-1 constructs on stem cell differentiation (35–37). In the current study, we have successfully isolated a high affinity anti-hCyclinT1 sFv clone (3R6-1) that can specifically bind to its cellular target protein *in vivo* and have a significant inhibitory effect on HIV-1 replication without apparent toxicity. Our results indicate that the sFv 3R6-1 clone could be very useful for HIV-1 gene therapy studies. Accordingly, it will be important to assess the *in vivo* biological effects of 3R6-1 and other new anti-hCyclinT1 intrabodies on stem cell differentiation and HIV-1 replication in this small animal model as a first step in our pre-clinical studies.

Acknowledgments—We thank Dr. Peterlin, who kindly provided us with GST-hT1 expression vectors, Dr. Kathy Jones, who kindly provided hCyclinT1 pCI-84 vector, and the National Institutes of Health AIDS Research and Reference Reagent Program that provided Jurkat and SupT1 cell lines and HIV-1 virus strains.

REFERENCES

1. Emerman, M., and Malim, M. H. (1998) *Science* **280**, 1880–1884
2. Price, D. H. (2000) *Mol. Cell. Biol.* **20**, 2629–2634
3. Peng, J., Zhu, Y., Milton, J. T., and Price, D. H. (1998) *Gene & Dev.* **12**, 755–762
4. Yang, Z., Zhu, Q., Luo, K., and Zhou, Q. (2001) *Nature* **414**, 317–322
5. Nguyen, V. T., Kiss, T., Michels, A. A., and Bensaude, O. (2001) *Nature* **414**, 322–325
6. Bieniasz, P. D., Gridina, T. A., Bogerd, H. P., and Cullen, B. R. (1999) *Mol. Cell. Biol.* **19**, 4592–4599
7. Jones, K. A. (1997) *Genes Dev.* **11**, 2593–2599
8. Wei, X., Ghosh, S. K., Taylor, M. E., Johnson, V. A., Emini, E. A., Deutsch, P., Lifson, J. D., Bonhoeffer, S., Nowak, M. A., Hahn, B., Saag, M. S., and Shaw, G. M. (1995) *Nature* **373**, 117–122
9. Karn, J. (1999) *Tackling Tat. J. Mol. Biol.* **293**, 235–254
10. Fujinaga, K., Taube, R., Wimmer, J., Cujec, T. P., and Peterlin, B. M. (1999)

- Proc. Natl. Acad. Sci. U. S. A.* **96**, 1285–1290
11. Fong, Y. W., and Zhou, Q. (2001) *Nature* **414**, 929–933
 12. Mhashilkar, A., Bagley, J., Chen, S. Y., Szilvary, A. M., Helland, D. G., and Marasco, W. A. (1995) *EMBO J.* **14**, 1542–1551
 13. Marasco, W. A., LaVecchio, J., and Winkler, A. (1999) *J. Immunol. Methods* **231**, 223–238
 14. Hoogenboom, H. R. (2000) *Immunol. Today* **21**, 371–378
 15. Winter, G., Griffiths, A. D., Hawkins, R. E., and Hoogenboom, H. R. (1994) *Annu. Rev. Immunol.* **12**, 433–455
 16. Harrison, J. L., Williams, S. C., Winter, G., and Nissim, A. (1996) *Methods Enzymol.* **267**, 83–109
 17. Popovic, M., Sarngadharan, M. G., Read, E., and Gallo, R. C. (1984) *Science* **224**, 497–500
 18. Garber, M. E., Wei, P., KewalRamani, V. N., Mayall, T. P., Herrmann, C. H., Rice, A. P., Littman, D. R., and Jones, K. A. (1998) *Genes & Dev.* **12**, 3512–3527
 19. Caputo, A., Sodroski, J. G., and Haseltine, W. A. (1990) *J. Acquired Immune Defic. Syndr.* **3**, 372–379
 20. Hauber, J., Malin, M. H., and Cullen, B. (1989) *J. Virol.* **63**, 1181–1187
 21. Desrosier, R. (1999) *Nat. Med.* **5**, 723–725
 22. Wei, P., Garber, M. E., Fang, S. M., Fischer, W. H., and Jones, K. A. (1998) *Cell* **92**, 451–462
 23. Ho, D. D., Neumann, A. U., Perelson, A. S., Chen, W., Leonard, J. M., and Markowitz, M. (1995) *Nature* **373**, 123–126
 24. Mhashilkar, A. M., Biswas, D. K., La Vecchio, J., Pardee, A. B., and Marasco, W. A. (1997) *J. Virol.* **71**, 6486–6494
 25. Zhou, C., Bahner, I., Larson, G. P., Zaia, J. A., Rossi, J. J., and Kohn, D. B. (1994) *Gene (Amst.)* **149**, 33–39
 26. Lee, N. S., Dohjima, T., Bauer, G., Li, H., Li, M.-J., Ehsani, A., Salvaterra, P., and Rossi, J. (2002) *Nat. Biotech.* **19**, 500–505
 27. Cafaro, A., Caputo, A., Fracasso, C., Maggiorella, M. T., Goletti, D., Baroncelli, S., Pace, M., Sernicola, L., Koanga-Mogtomo, M. L., Betti, M., Borsetti, A., Belli, R., Akerblom, L., Corrias, F., Butto, S., Heeney, J., Verani, P., Titti, F., and Ensoli, B. (1999) *Nat. Med.* **5**, 643–650
 28. Korber, B., Kuiken, C., Foley, B., Hahn, B., McCutchan, F., Mellors, J., and Sodroski, J. (1998) *HIV Sequence Database Theoretical Biology and Biophysics (T10)*, Los Alamos National Laboratory, Los Alamos, NM
 29. Morrison, S., Uchida, N., and Weissman, I. (1995) *Annu. Rev. Cell Dev. Biol.* **11**, 35
 30. McCune, J. M., Namikawa, R., Kaneshima, H., Shultz, L. D., Lieberman, M., and Weissman, I. L. (1988) *Science* **241**, 1632–1639
 31. Jamieson, B., Aldrovandi, G. M., and Zack, J. A. (1996) *Semin. Immunol.* **8**, 215–221
 32. Kollmann, T. R., Pettoello-Mantovani, M., Zhuang, X., Kim, A., Hachamovitch, M., Smarnworawong, P., Rubinstein, A., and Goldstein, H. (1994) *J. Exp. Med.* **179**, 513–522
 33. Brooks, D. G., and Zack, J. A. (2002) *J. Virol.* **76**, 1673–1681
 34. Brooks, D. G., Kitchen, S. G., Kitchen, C. M. R., Scripture-Adams, D. D., and Zack, J. A. (2001) *Nat. Med.* **7**, 459–464
 35. Bai, J., Gorantla, S., Banda, N., Cagnon, L., Rossi, J., and Akkina, R. (2000) *Mol. Ther.* **1**, 244–254
 36. Bai, J., Banda, N., Rossi, J., and Akkina, R. A. (2002) *Mol. Ther.*, in press
 37. Banda, N., Akkina, R. K., Terrell, K., Shpall, E. J., Tomczak, J., Campaign, J., Clamam, H., Cagle, L., and Harrison, G. S. (1998) *J. Hematother.* **7**, 319–331